Extension of the Common Image Gathers by VPRTM method

*Gennady Erokhin**, *Aleksandr Danilin and Maksim Kozlov, Immanuel Kant Baltic Federal University*

Summary

The process of scattering the acoustical wave on an obstacle at any moment of time may be considered as an interaction of two interconnected vectors: the particle velocity vector of the incident wave and generated by scattering the vector of the reflected or scattered wave. Mathematical method of the inversion the wave front in time, based on the first order differential equations allows investigating such interaction more carefully. Proposed Vector Pair Reverse Time Migration method demands large storage memory and high computer performance but provides the new opportunities for studying the environment.

Introduction

The Reverse Time Migration (RTM) image processing (Baysal et.al.,1983; Whitmore, 1983; McMechan, 1983) is wide used for the constructing the Angle Domain Image Gathers (ADCIG). The method RTM has the own internal artefacts because the method is based on the wave-equation. For overcoming such artefacts the image regularization is performed by filtration in an extended spaces of angle parameters (Yoon and Marfurd, 2006; Sava and Fomel, 2006; Zhang and McMechan, 2011). Despite the growing the performance of computer, there exist opinions, that using the RTM in full extended spaces is still very expansive (Vyas et.al., 2011, Guan et.al., 2013). Nevertheless Erokhin et.al., 2017 suggested the new Vector Pair Reverse Time Migration (VPRTM) method, which really demands relatively large memory and high computer performance, but it seems that method provides the new opportunities for studying the subsurface environment.

In this paper we propose the new conception of the extraction and regularization, by the VPRTM method, of information for CIG, which allows us to create new subsurface images based on the new Imaging Conditions. We illustrate our approach by the model and the real experiment.

Method

The mathematical statement VPRTM derives acoustical wave by the couple $(p,\vec{u})$ where p is the pressure and $\vec{u}$ is the particle velocity vector field, which satisfy the first order linear differential equations.

$$\begin{aligned} &p^f{}_t - \rho c^2 div(\nabla \vec{u}^f) = r(t)\delta(x - x_s) \\ &\rho \vec{u}^f_t = \nabla p^f \\ &p^f\big|_{t=0} = 0, \quad \vec{u}^f\big|_{t=0} = 0. \end{aligned} \tag{1}$$

Here $r(t)\delta(x-x_s)$ is the source located at the boundary point $x_s \in \Gamma = \left\{ x \in \mathbb{R}^n \middle| x^n = 0,\ n = 2,3 \right\}$ (δ is the Dirac function, and r is some wavelet), T is the time of observation. Let $p_0 = p^f\big|_{\Gamma\times[0,T]}$ be the "measured" pressure, $c = c(x)$ - medium velocity, $\rho = \rho(x)$ density (for simplicity, further we set the density equal to 1. The adjoint problem to the problem (1) is written as follows

$$\begin{aligned} &p^b{}_t - \rho c^2 div(\nabla \vec{u}^b) = 0 \\ &\rho \vec{u}^b_t = \nabla p^b + p_0 \delta(x^n)\vec{\nu}_\Gamma \\ &p^b\big|_{t=T} = 0, \quad \vec{u}^b\big|_{t=T} = 0, \end{aligned}$$

(2)

where $\nu_\Gamma = (0,...0,1)$) is the unit normal vector to Γ. We call $(p^b, \vec{u}^b)$ the back wave since it propagates in reversal time. So, forward and back waves, except pressure, include two vector fields: $\vec{u}^f(x,t;x_s)$ and $\vec{u}^b(x,t;x_s)$. Further we will use short notations $f = \vec{u}^f$, $b = \vec{u}^b$.

The typical behavior of the interconnected vector pair (IVP) (f,b) at some fixed x, located, for example, at the boundary of two half-spaces with velocity $3km/s$, (upper) and $3.1km/s$ (down) for a fixed x_s is presented at Fig. (1a,1b). The same for the point x, coincided with point of diffraction (where the velocity $3.1km/s$) and backgroud velosity $3km/s$ is presented at Fig. (1a,1c).

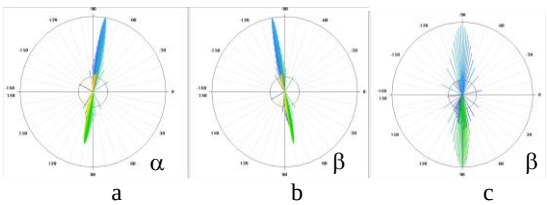

Figure 1: Incident and scattering behaviour of interconnected vector par (f,b) for the point of reflection (a), (b) and for the

10.1190/segam2018-2995971.1

point of diffraction (a),(c). Here α is the incident angle, β is the scattering angle.

RTM-based Angle Domain Common Image Gathers (ADCIG) usually uses the pressure (Baisal et.al., 1983). The angles of incident and scattering waves are calculated additionally using, for example, Poynting vector which, sometimes, is accumulated on time (Yoon and Marfurd, 2006). The result of such approach is obtaining the two values of average pressures and the two values of average angles near meeting time of forward and back waves. Is there exist the another, more detail and more informative approach for designing a undersurface gather similar ADCIG? The answer is yes, if we will use the first order linear differential equations (1)–(2) and will be calculate not only pressure but the velocity vector too.

Really, let Q be set of vectors $Q=\{\vec{p}_k\}\quad k=1,...,N\quad N=N_T\times N_s$, where N_T - number of time sampling, N_s - number of sources, $\vec{p}=(t,s,|f|,\|b|,\gamma,\theta,p^f,p^b,\omega_f,\omega_b)$ is a vector from R^8, $\gamma=(\alpha-\beta)/2$ is opening angle , $\theta=(\alpha+\beta)/2$ is the dip angle, ω_f, ω_b are the instantaneous circular frequency of rotation of the vectors f and b (Hz, clockwise positive, versus negative).

Let denote such set Q as Vector Domain Common Image Gather (VDCIG). So, for each point of acoustic media the set of vectors $\vec{p}_k$ statistically describes the main characteristics of the forward and the back waves. It is very important to underline that the all components of the each vector $\vec{p}_k$ are interconnected. That is main prerequisite to design the Imaging Condition (IC) based on VDCIG as Interconnected Vector Pair Imaging Condition (IVP IC). The procedure of constructing the image consists of the two stages. At the first stage we search the admissible subset $Q_P\subseteq Q$. Subset is the result of filtration (regularization) the full set Q by not only restrictions of set $\{t_k,x_s|k=0,...,N_T,\in t\in[0,T],s=1,...,N_s\}$, but else by restriction of remaining components of vector $\vec{p}=(t,s,|f|,\|b|,\gamma,\theta,p^f,p^b,\omega_f,\omega_b)$, which will be belong to admissible subset $Q_P\subseteq Q$. For example, such subset is

$$Q_P=\{\vec{p}\,|(<b,f>/|b|\,|f|)\le c\le 1\} \qquad (3)$$

where $<,>$ means scalar product and "c" some constant. The regularization (3) is similar to approach by Stolk et.al., 2009, Whitmore and Crawley, 2012. The designing of the admissible subset Q_P with angle-domain (α,β) or (θ,γ) restrictions is similar to the filtration on the basis of local image matrix (Xie and Wu, 2002; Yan and Xie, 2009).

scattering angle. Color shows the time from blue up At the second stage of constructing the image we choose the concrete type of IVP IC, which is written in common form as follows:

$$I(x)=R_{Q_P}(\vec{p})(x), \qquad (4)$$

where R_{Q_P} is some operator defined on the subset $Q_P\subseteq Q$ being applied to the pair of vectors (f,b) or to the pair of pressures (p^f,p^b) from subset Q_P. Such operator may be product, scalar product, product of modules of two vectors, division, phase operation etc., with subsequent summation or calculation of averages or variances (Erokhin et. al., 2017). For example,the operator:

$$R_{Q_P}=\sum_Q(p^f\,p^b) \qquad (5)$$

is exactly conventional RTM. For the velocity vectors (f,b) the similar operator is:

$$R_{Q_P}=\sum_Q(|f\,\|b\|) \qquad (6)$$

The Imaging Condition (6) coincides with the impedance imaging, up to a density factor.

Synthetic Data Example

For simplicity, we will consider two-dimensional case. To solve Cauchy problems (1) - (2), we use the finite-difference time domain method with staggered grids in space and time. The spatial derivatives are approximated with 12th accuracy order and time derivatives have second accuracy order. The modeling parameters are the following: the whole computational domain is $17\times3.5\,km$, the spacing step is $5\,m$ the number of sources is 200, the source step is $50\,m$ the computational domain for one source is $7\times3.5\,km$, the number of receivers is 701, the receiver interval is $10\,m$, the time step is $0.4\,ms$, $r(t)$ is Ricker's wavelet with dominant frequency $40\,Hz$.

The filtration based on the condition (3) is popular for removing noise which connect with the nature of RTM (Ren et.al., 2013). Another application of filtration (3) is connected with obtaining the Diffractivity Imaging (Koren and Ravve, 2011, Moser and Howard, 2008). The model with single difractor, which is located at the point with coordinates x=8500 m, z=1750 m is presented at the Fig. 2.

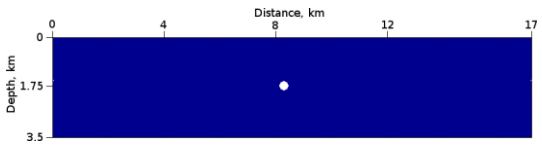

Figure 2: Model with single diffractor.

10.1190/segam2018-2995971.1

The (θ,γ) - distribution of the module of vectors $|b_k|$ at the diffraction point is described at Fig. 3a. The typical filtration of the reflected waves with cut-off parameter c=0.95 for condition (3) is presented at the Fig. 3b.

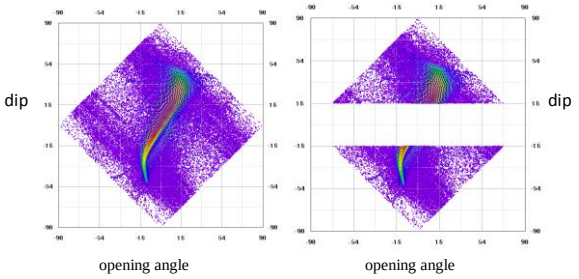

Figure 3: (θ,γ) - distribution of $|b_k|$ at the diffraction point before filtration (a) and after filtration (b). Color from blue up to red shows intensity of $|b_k|$

The Fig. 4 presents the IC (4) with operator (5) in form:

$$I(x) = R_{Q_+} + R_{Q_-} \quad R_{Q_{+-}} = \sum_{k_s=1}^{N_s}\sum_{k_t=1}^{N_t} (p^f p^b)_{k_s,k_t} Q = Q^{+-} \quad , (7)$$

where:

$$Q_+ = \{t_k, x_s \,|\, (\alpha\,\beta) > 0,\ k = 0,...,N_T,\ s = 1,...,N_s\}$$

$$Q_+ = \{t_k, x_s \,|\, (\alpha\,\beta) < 0,\ k = 0,...,N_T,\ s = 1,...,N_s\}$$

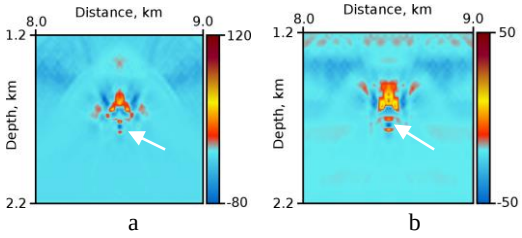

Figure 4: The images of the diffractor before filtration (a) and after 1D filtration (3) - (b).

So, the conventional approach to filtration of the reflected waves, based on regularization (3) is, in fact, 1D filter. At the same time the VPRTM approach allows us to obtain the more perfect diffraction images using the 2D domain of angles (θ,γ) and the true 2D filter. At the Fig. 5 such filter and the image of diffractor are presented. Note, that maximum amplitudes at Fig. 4a and Fig. 5b are twice more than at Fig. 4b.

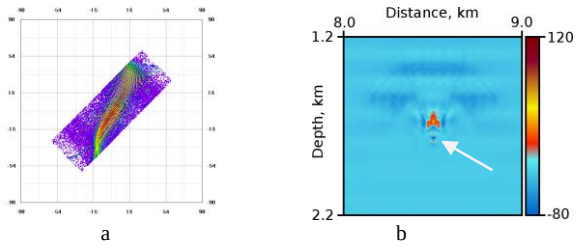

Figure 5: (θ,γ)-angle distribution of $|b_k|$ at the diffraction point after 2D filtration (a) and the image of the diffractor after 2D filtration (b).

Further, if the IC (7) has the operator of the form $R_{Q_P} = R_{Q_P}(|b|)$ then after 2D filtration (Fig. 5a) the image of diffractor looks like on the Fig. 6a. For the case, when the operator R_{Q_P} has the type (6) the image of diffractor looks like on the Fig. 6b.

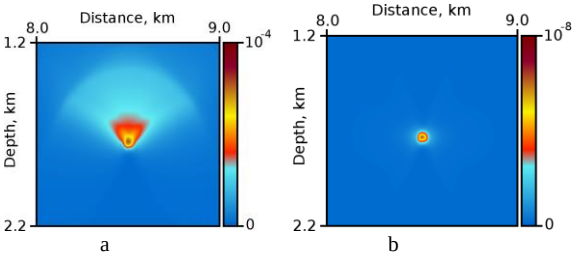

Figure 6: Images of the diffractor for $R_{Q_P} = R_{Q_P}(|b|)$ in formula (7) - (a) and for $R_{Q_P} = R_{Q_P}(|b||f|)$ in formula (7) - (b)

All images, above mentioned, use only amplitude informatin in IC (4). At the same time it is very intresting to use the information directly about phase, more specifically about dip θ , about opening angle γ or about some other parameters**.** Let the operator R_{Q_P} has the form:

$$R_{Q_\theta} = M(\theta_{k_s,k_t}),\ \theta_{k_s,k_t} \in Q_P \quad k_t = 0,...,N_T, k_s = 1,...,N_s \ , \quad (8)$$

$$R_{Q_\gamma} = M(\gamma_{k_s,k_t}),\ \gamma_{k_s,k_t} \in Q_P \quad k_t = 0,...,N_T, k_s = 1,...,N_s \ , \quad (9)$$

where M is the mathematical expectation. Then the images of phase distributon near the point of diffraction are shown at Fig.7.

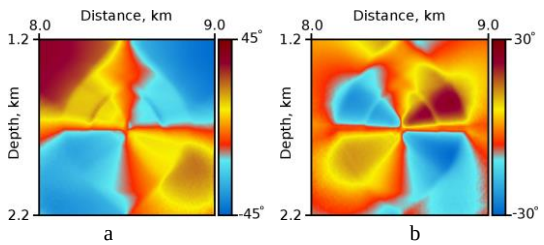

Figure 7: Mathematical expectations of dip θ (a) and opening angle γ (b)

10.1190/segam2018-2995971.1

A similar representation of the operator R_{Q_p} at the form (8) or (9), but for the AVO parameters Intercept or Gradient gives the images showed at Fig. 8. The results of similar calculations for Instantaneous Frequency of rotation of the vector b and number of source S give the images, showed at Fig. 9.

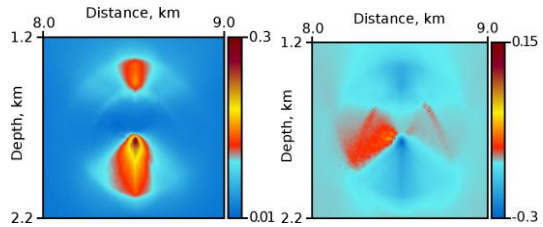

Figure 8: Mathematical expectations of the Intercept (a) and the Gradient (b)

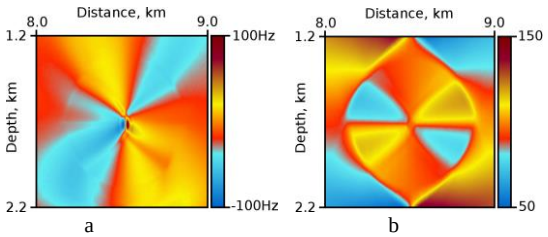

Figure 9: Mathematical expectations of the Instantaneous Frequency ϖ_b (a) and the number of source S.

Field Data Example

The new possibilities of the VPRTM method and the of the VDCIG conception are presented below on the example of the oilfield in the West Siberia. Fig.10a shows the result of conventional RTM processing with IC form (6) (similarly Fig. 6b). Fig 10b demonstrate VPRTM processing with IC like (7), but where $I(x) = R_{Q_+} - R_{Q_-}$ and $R_{Q+-} = R_{Q+-}(|b|)$. We named last case the BackRTM. The impedance, calculated according formula (7) with the same operator $R_{Q+-} = R_{Q+-}(|b|)$ is showed at Fig. 11a (similarly Fig.4 and Fig.5b). Soft (blue) and Hard (brown) diffraction are presented at Fig.11b. Mathematical expectations of dip θ (a) and opening angle γ (b) are showed at Fig. 12 (similarly Fig.7). The distribution of instantaneous frequency of the vector rotation b in Hz (clockwise positive, versus negative) is presented on Fig. 13a (like on Fig. 9a). Fig. 13b shows the AVO Fluid Factor.

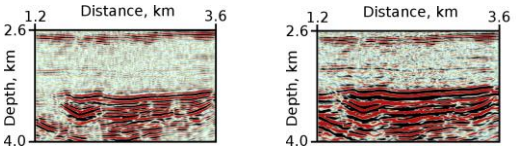

Figure 10: RTM (a) and BackRTM (b)

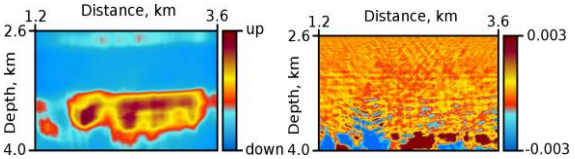

Figure 11: Impedance (a) and Soft (blue) and Hard (brown) Diffraction (b)

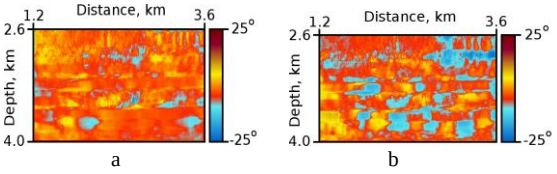

Figure 12 : Dip (a) and Opening Angle (b)

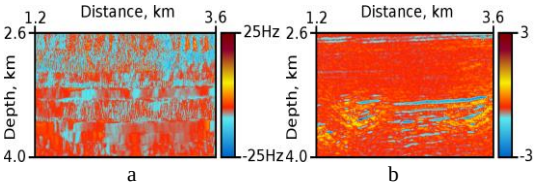

Figure 13: Instantaneous frequency of the vector rotation b (clockwise positive, versus negative) - (a) and AVO Fluid Factor - (b)

Conclusion and Discussion

The distinctive feature of the proposed VPRTM method is incorporation the velocity vector in procedure of extraction the information for designing extended CIG. Proposed Vector Domain CIG contain essentially more information and more possibility regularization of image processing. The method introduces higher requirements to the hardware, but it makes it possible to calculate many interesting attributes simultaneously. Especially this is concern with the phase attributes. The new suite of attributes, calculated simultaneously, gives us the good perspective to interpret obtained information together, using a powerful statistical tool.

Acknowledgments

This work is supported by the Russian Science Foundation under grant 16-11-10027.

10.1190/segam2018-2995971.1

REFERENCES

Baysal, E., D. D. Kosloff, and J. W. C. Sherwood, 1983, Reverse time migration: Geophysics, **48**, 1514–1524, https://doi.org/10.1190/1.1441434.

Erokhin, G., L. Pestov, A. Danilin, M. Kozlov, and D. Ponomarenko, 2017, Interconnected vector pairs image conditions: New possibilities for visualization of acoustical media: 87th Annual International Meeting, SEG, Expanded Abstracts, 4624–4629, https://doi.org/10.1190/segam2017-17587902.1.

Guan, H., P. Williamson, B. Denel, F. Audebert, and B. Duquet, 2013, Angle-domain common-image gathers extracted from pre-stack RTM images: 83rd Annual International Meeting, SEG, Expanded Abstracts, 3767–3772, https://doi.org/10.1190/segam2013-1149.1.

Koren, Z., and I. Ravve, 2011, Full-azimuth subsurface angle domain wavefield decomposition and imaging Part 1: Directional and reflection image gathers: Geophysics, **76**, no. 1, S1–S13, https://doi.org/10.1190/1.3511352.

McMechan, G. A., 1983, Migration by extrapolation of time-dependent boundary values: Geophysical Prospecting, **31**, 413–420, https://doi.org/10.1111/j.1365-2478.1983.tb01060.x.

Moser, T. J., and C. B. Howard, 2008, Diffraction imaging in depth: Geophysical Prospecting, **56**, 627–641, https://doi.org/10.1111/j.1365-2478.2007.00718.x.

Ren, L., G. Liu, X. Meng, J. Wang, and S. Zhang 2013, Suppressing artifacts in 2D RTM using the Poynting vector: Near Surface Geophysics Asia Pacific Conference, 484–487, https://doi.org/10.1190/nsgapc2013-112.

Sava, P., and F. Sergey, 2006, Time-shift imaging condition in seismic migration: Geophysics, **71**, no. 6, S209–S217, https://doi.org/10.1190/1.2338824.

Stolk, C. C., M. V. de Hoop, and T. Op't Root, 2009, Linearized inverse scattering based on seismic reverse-time migration: Proceedings of the Project Review, Geo-Mathematical Imaging Group, 91–108.

Vyas, M., D. Nichols, and E. Mobley, 2011, Efficient RTM angle gathers using source directions: 81st Annual International Meeting, SEG, Expanded Abstracts, 3104–3108, https://doi.org/10.1190/1.3627840.

Whitmore, N. D., 1983, Iterative depth migration by backward time propagation: 53rd Annual International Meeting, SEG, Extended Abstracts, 382–385, https://doi.org/10.1190/1.1893867.

Whitmore, N. D., and S. Crawley, 2012, Applications of RTM inverse scattering imaging conditions: 82nd Annual International Meeting, SEG, Expanded Abstracts, 1–6, https://doi.org/10.1190/segam2012-0779.1.

Xie, X., and R. S. Wu, 2002, Extracting angle domain information from migrated wavefields: 72nd Annual International Meeting, SEG, Expanded Abstracts, 1360–1363, https://doi.org/10.1190/1.1816910.

Yan, R., and X.-B. Xie, 2009, A new angle-domain condition for prestack reverse-time migration: 79th Annual International Meeting, SEG, Expanded Abstracts, 2784–2788, https://doi.org/10.1190/1.3255427.

Yoon, K., and K. J. Marfurt, 2006, Reverse-time migration using the Poynting vector: Exploration Geophysics, **37**, 102–107, https://doi.org/10.1071/EG06102.

Zhang, Q., and G. A. McMechan, 2011, Direct vector-field method to obtain angle-domain common-image gathers from isotropic acoustic and elastic reverse-time migration: Geophysics, **76**, no. 5, WB135–WB149, https://doi.org/10.1190/geo2010-0314.1.